NASA TECHNICAL NOTE

NASA TN D-7724

NASA TN D-7724

ANALYSIS OF AN ALL-METALLIC RESILIENT-PAD GAS-LUBRICATED THRUST BEARING

by William J. Anderson

Lewis Research Center

Cleveland, Ohio 44135

NATIONAL AERONAUTICS AND SPACE ADMINISTRATION • WASHINGTON, D. C. • JULY 1974

1. Report No. NASA TN D-7724	2. Government Accession No.	3. Recipient's Catalog No.
4. Title and Subtitle ANALYSIS OF AN ALL-METALLIC RESILIENT-PAD GAS-LUBRICATED THRUST BEARING		5. Report Date JULY 1974 6. Performing Organization Code
7. Author(s) William J. Anderson		8. Performing Organization Report No. E-7966 10. Work Unit No. 501-24
9. Performing Organization Name and Address Lewis Research Center National Aeronautics and Space Administration Cleveland, Ohio 44135		11. Contract or Grant No. 13. Type of Report and Period Covered Technical Note
12. Sponsoring Agency Name and Address National Aeronautics and Space Administration Washington, D.C. 20546		14. Sponsoring Agency Code

15. Supplementary Notes

16. Abstract

A new type of resilient-pad gas thrust bearing that does not contain any elastomers in the bearing assembly is described and analyzed. The bearing consists of sector-shaped pads mounted asymmetrically on resilient foil beams. The effects of bearing design parameters on performance are shown. Performance of a resilient-pad bearing is compared with that of a pivoted-pad bearing.

17. Key Words (Suggested by Author(s)) Bearings Gas bearings Thrust bearings Compliant bearings	18. Distribution Statement Unclassified - unlimited Category 15		
19. Security Classif. (of this report) Unclassified	20. Security Classif. (of this page) Unclassified	21. No. of Pages 32 34	22. Price* $3.25

* For sale by the National Technical Information Service, Springfield, Virginia 22151

ANALYSIS OF AN ALL-METALLIC RESILIENT-PAD GAS-LUBRICATED THRUST BEARING

by William J. Anderson

Lewis Research Center

SUMMARY

A new type of resilient-pad gas thrust bearing that does not contain any elastomers in the bearing assembly is described and analyzed. The bearing consists of sector-shaped pads mounted asymmetrically on resilient foil beams. Each pad deflects under load so as to form a load-supporting wedge of film. Equations for pad deflection are derived from the beam deflection equation and are used in conjunction with solutions for a compressibly lubricated flat slider to determine the operating characteristics of the resilient pad.

The procedure for determining the beam design for optimum load capacity at a specific operating condition together with the desired axial stiffness of the mount is described, and the results of computations for several combinations of design parameters are presented. Minimum film thicknesses of an optimized design are then determined for a range of operating speeds at several loads. The performance of a resilient-pad bearing is equal to that of a pivoted-pad bearing at its design point and has only a slightly lower film thickness at speeds above and below the design speed.

The advantages of the resilient-pad bearing, that is, greater tolerance to dirt ingestion, good initial lift-off characteristics, and operating capability over a wide temperature range, can thus be utilized with very little performance penalty.

INTRODUCTION

One of the problems encountered in the development and application of gas bearings is their sensitivity to contaminant particles, such as dirt, in the gas because they operate with small film thicknesses. In addition, the materials used in gas bearings generally have poorer tolerance to the ingestion of dirt. Gas bearing materials are harder, because of the high precision required, and have poorer embeddability than do the materials

used in conventional hydrodynamic bearings. These two factors - thinner films and hard face materials - combine to make rigid-geometry gas bearings very sensitive to contaminants.

The general approach taken to make gas bearings more tolerant to dirt ingestion is to develop bearings with flexible or compliant geometries, which prevent localized loading of the bearing surface, in place of conventional rigid-surface-geometry bearings. Considerable work has been done on foil bearings (refs. 1 to 4). In references 3 and 4 successful applications of foil bearings to high-speed turbomachines are reported. Foil bearings of both the tensioned type (refs. 2 and 3) and the overlapping cantilevered type (ref. 4) have been more successful as journal bearings than as thrust bearings.

Gas bearings with compliant surfaces of rubberlike material are also being considered. Originally developed for marine applications (refs. 5 and 6), rubber-face bearings have recently been the subject of several investigations as gas bearings (refs. 7 to 10). They have some interesting properties and indicate promise, but they are temperature limited because of the presence of an elastomeric material.

Bearings with rigid-geometry load-carrying surfaces, but with one of the load-carrying elements (such as pads or steps) mounted on a compliant backing, are also being investigated (ref. 11 and unpublished data from Shapiro, Chu, and Kramberger of Franklin Institute Research Laboratories). Shapiro and coworkers report success with thrust bearings having rigid, graphitic-carbon pads in which the pads are mounted on a rubber back. This bearing performs well but is again temperature limited by the presence of an elastomer.

The bearing concept analyzed in this report was conceived with two objectives in mind: to provide a bearing with better tolerance to dirt ingestion by incorporating compliance or resilience into the bearing structure and to accomplish this with all-metallic components, which would make the bearing suitable for high-temperature operation. The concept, as applied to a thrust bearing, consists of a number of rigid, sector-shaped pads, each mounted asymmetrically on a flexible beam between radial spokes which act as supports. A schematic of a resilient-pad bearing with six pads is shown in figure 1.

SYMBOLS

a length of flexible beam from trailing edge of pad to support, cm; in.

b length of flexible beam from support to leading edge of pad, cm; in.

E Young's modulus of beam material, N/m^2; psi

h_1 film thickness at inlet to pad, cm; in.

h_2 film thickness at exit from pad, cm; in.

I	moment of inertia of flexible beam, $\left[(R_o - R_i)/12\right] t^3$, m^4; $in.^4$
K_m	flexible beam stiffness, N/m; lb/in.
K_1, K_2	beam load reaction coefficient, N; lb
l	length of pad in direction of motion, cm; in.
$M_1, M_2, M_3,$ M_4, M_{5L}, M_{5R}	moments acting on flexible beam, (N)(m); (lb)(in.)
N	rotative speed of slider, rpm
P	pad load, N; lb
p_a	ambient pressure, N/m^2; psi
R_i	radius to inside of pad, cm; in.
R_m	mean radius of pad, $(R_o - R_i)/2$, cm; in.
R_o	radius to outside of pad, cm; in.
S_2	location of center of pressure on pad, cm; in.
t	thickness of flexible beam, mm; in.
v	sliding velocity at R_m, $2\pi R_m N/60$, cm/sec; in./sec
x, y	coordinates for determining beam deflection
δ_a, δ_b	beam deflections, m; in.
θ	pad slope in direction of motion, rad
Λ	bearing characteristic number, $6\mu v l/p_a h_2^2$
μ	dynamic viscosity of gas, (N)(sec)/m^2; (lb)(sec)/$in.^2$

ANALYSIS

The bearing analyzed is a thrust bearing which consists of several rigid, sector-shaped pads, each mounted on the same flexible foil plate. The foil plate is mounted in turn on a supporting structure consisting of radial spokes. Each pad is located asymmetrically between the radial spokes. Each foil plate sector between radial spokes is considered to be a flexible beam. The beams can be mounted on the radial spokes with either simple supports (no constraint on the beam slope at each spoke) or constrained supports (the beam slope constrained to be zero at each spoke). A schematic of a single pad and beam arrangement with simple supports is shown in figure 2(a), and a schematic of a pad and beam with constrained supports is shown in figure 3(a).

Equations for the slope of the pad and for the axial stiffness of the pad mount were developed from beam theory for the two cases: simple and constrained supports. Free-body diagrams for the beam and pad with simple supports are shown in figures 2(b) and (c), and those for the beam and pad with constrained supports are shown in figures 3(b) and (c). Appendix A outlines the derivation of the equations for pad slope and pad mount axial stiffness for the case of simple supports, and appendix B for the case of constrained supports. For each case the slope and stiffness are functions of the beam asymmetry b/a, the beam elastic constant EI, the pad dimension in the direction of motion l, the pad load P, and the location of the center of pressure on the pad S_2/l.

These equations are solved simultaneously with the compressible-flow Reynolds equation applied to a flat slider to obtain the operating characteristics of a pad mounted on a flexible beam. As an initial approach a bearing geometry utilizing a square pad was chosen so that published solutions which define the performance of a compressibly lubricated square pad could be used.

The bearing geometry chosen for design and the procedure followed for optimizing the design parameters for a given operating condition are given in the next section. Finally, the steps followed to determine the operating characteristics of the bearing over a range of operating speeds are outlined, and an example is presented.

DESIGN PROCEDURE

A six-pad bearing having the following dimensions was chosen for the design:

Radius to outside of pad, R_o, cm (in.)	4.75 (1.75)
Radius to inside of pad, R_i, cm (in.)	2.54 (1.00)
Length of pad in direction of motion, l, cm (in.)	1.91 (0.75)
Length of flexible beam, a + b, cm (in.)	1.75 (0.69)
Ambient pressure, p_a, N/m^2 (psi)	1×10^5 (14.7)
Dynamic viscosity of gas, μ, (N)(sec)/m^2 ((lb)(sec)/$in.^2$)	1.86×10^{-5} (2.7×10^{-9})
Mean radius of pad, R_m, cm (in.)	3.49 (1.375)

In the design procedure the assumption is made that the sector-shaped pad behaves as a rectangular pad with a length in the direction of motion l equal to the arc length along the mean radius R_m and a width normal to the direction of motion equal to $R_o - R_i$. Beam dimensions a and b are also taken along the mean radius R_m, and beam width is taken as $R_o - R_i$. The velocity of sliding v is calculated along the mean radius R_m.

DESIGN OPTIMIZATION

The first step was to determine the design parameters for optimum operation at a given Λ. A Λ value of 40 was chosen because curves of dimensionless load $P/\Lambda p_a l(R_o - R_i)$ as a function of film thickness ratio h_1/h_2 were available in reference 12 for Λ values of 1, 10, and 40. A Λ value of 40 represents a reasonable pad load. The curves of reference 12 are shown in figure 4. For optimum load capacity at $\Lambda = 40$ (maximum value of dimensionless load) $h_1/h_2 = 3.6$. The pad load is then 11.5 newtons (2.58 lb). This value represents a pad load pressure of 3.19×10^4 newtons per square meter (4.59 psi). The location of the center of pressure S_2/l for $\Lambda = 40$ and $h_1/h_2 = 3.6$ is obtained from figure 5 (ref. 12).

Everything required to solve for the pad slope θ for a chosen set of values of b/a, E, and I is now known. Equation (A20) is used for simple supports and equation (B22) for constrained supports. From geometry

$$\theta \cong \frac{h_1 - h_2}{l} = \left(\frac{h_1}{h_2} - 1\right)\frac{h_2}{l}$$

The value of h_2 is calculated and used to determine the rotative speed N from the bearing characteristic number Λ

$$N = \frac{10\Lambda p_a h_2^2}{2\pi R_m \mu l}$$

The operating speeds N for optimum operation at various values of beam thickness t and length ratio b/a were determined for both simple and constrained supports at three values of Λ. These results are listed for constrained supports in table I and for simple supports in table II.

The results for three values of t and values of b/a from 1.2 to 2.0 for constrained supports are plotted in figure 6. The beam material is molybdenum ($E = 3.47\times10^{11}$ N/m^2 (50×10^6 psi)). The design parameters chosen for the bearing were $t = 0.254$ millimeter (0.010 in.) and $b/a = 1.7$. These values result in optimum load capacity at $N = 25\,000$ rpm for a pad load pressure of 3.19×10^4 newtons per square meter (4.59 psi).

The procedure for determining the mount axial stiffness K_m, which must be known to calculate axial resonances, is quite similar; K_m is calculated for simple supports by using equations (A21) and (B23). The results for constrained supports are shown in figure 7. The axial stiffness is almost a pure function of t, the beam thickness. It is almost independent of b/a. Curves are shown for $\Lambda = 1$ as well as for $\Lambda = 40$; they indicate very little dependence on load over the range investigated.

The results obtained for simple supports are almost identical with those for constrained supports, and for that reason are not shown. Figure 8 shows minimum film thickness as a function of speed for both bearing types.

OPERATING CHARACTERISTICS AT CONSTANT LOAD

After designing a bearing for optimum load capacity at a given speed and pad load, it was necessary to determine its operating characteristics over a range of operating speeds. To do this, it was necessary to interpolate among the Λ values of 1, 10, and 40 to establish curves such as those of figure 4 for other values of Λ. It is recognized that this is an approximate procedure. The more accurate procedure would be to obtain numerical solutions to the compressible flow Reynolds equation at the desired Λ values. This is a tedious and expensive approach, however, and one not considered warranted until a thorough experimental evaluation of the concept is completed.

Values of P were chosen which will result in intercepts of the dimensionless load parameter $P/\Lambda p_a l(R_o - R_i)$ with curves of constant Λ such as those of figure 4. For each intercept a value of h_1/h_2 is obtained. Values of S_2/l are obtained from curves such as those in figure 5. As before, this yields the information required to solve for θ and h_2. A value of N at each intercept point in figure 4 can then be calculated.

Results for both simple and constrained supports at two load values are listed in tables III and IV. Figure 9 shows a plot of minimum film thickness as a function of speed for the constrained support bearing at three pad load values.

Figure 4 shows the operating line for the optimized bearing design at P = 9.46 newtons (2.13 lb). This corresponds to a pad load pressure of 2.63×10^4 newtons per square meter (3.79 psi). Before startup, if the pad is loaded, the deflection characteristics are such that the runner touches the pad at its trailing edge and $h_1/h_2 = \infty$. When rotation of the runner ensues, lift-off occurs and h_1/h_2 quickly drops to a finite value. Points on the bearing operating line indicate where the bearing operates at different speeds. With increasing speed h_1/h_2 decreases because of greater lift-off. Optimum operation is at a speed of approximately 25 000 rpm.

Figure 10 shows the operating line for the optimized bearing design at P = 4.05 newtons (0.91 lb), which corresponds to a load pressure of 1.12×10^4 newtons per square meter (1.62 psi). Note that optimum operation occurs at a speed of 3060 rpm. The lower the load, the more quickly the pad lifts off and reaches its optimum operating condition.

COMPARISON WITH A PIVOTED-PAD BEARING

A resilient-pad bearing resembles a pivoted-pad bearing in the way it functions, so a comparison of its operating characteristics with those of a similar pivoted-pad bearing is of interest. Figure 11 shows a plot of minimum film thickness as a function of speed for both bearing types. A pivot position of 0.685 was chosen for the pivoted-pad bearing to give optimum performance at the design point for which the resilient-pad bearing was optimized. As expected, the performance of both bearings at the design point is identical. At speeds above and below the design point, the pivoted-pad bearing is slightly superior. The differences in film thickness are quite small over a wide speed range, however. This indicates that the potential advantages of the resilient-pad bearing, such as greater tolerance to dirt ingestion, good initial lift-off characteristics, and operating capability over a wide temperature range, can be utilized with only a small sacrifice in performance.

SUMMARY OF RESULTS

The procedure for optimizing the design of an all-metallic resilient-pad gas-lubricated thrust bearing for operation at a given set of design conditions was shown to be straightforward. The operating characteristics of an optimized bearing design were determined for a range of operating speeds. The performance of a resilient-pad bearing was equal to that of a pivoted-pad bearing at its design point with only a slightly lower film thickness at speeds above and below the design speed. The advantages of the resilient-pad bearing, that is, greater tolerance to dirt ingestion, good initial lift-off characteristics, and operating capability over a wide temperature range, could thus be utilized with very little performance penalty.

Lewis Research Center,
National Aeronautics and Space Administration,
Cleveland, Ohio, May 13, 1974,
501-24.

APPENDIX A

DERIVATION OF PAD SUPPORT BEAM DEFLECTION AND AXIAL STIFFNESS FOR SIMPLE SUPPORTS

From figure 1 the boundary conditions are

(1) At $x = 0$, $dy/dx = \theta$.

(2) At $x = 0$, $y = \delta_b - \delta_a$.

(3) At $x = a$, $y = \delta_b$.

(4) At $x = a + b$, $dy/dx = \theta$.

(5) At $x = a + b$, $y = 0$.

(6) At $x = a$, $(dy/dx)_{x=a-\Delta x} = (dy/dx)_{x=a+\Delta x}$, where $\Delta x \to 0$.

For the entire beam

$$M_1 - M_2 - (1 - K_1)Pa + K_1Pb = 0 \tag{A1}$$

For the pad

$$K_1PS_2 + M_2 - M_1 - (1 - K_1)(\ell - S_2)P = 0 \tag{A2}$$

From equations (A1) and (A2)

$$K_1 = \frac{\ell + a - S_2}{a + b + \ell} \tag{A3}$$

For the beam from $x = 0$ to $x = a$

$$M = M_1 - (1 - K_1)Px \tag{A4}$$

From $x = a$ to $x = a + b$

$$M = M_1 - (1 - K_1)Px + P(x - a) \tag{A5}$$

Using the well known equation for beam deflection

$$EI\frac{dy^2}{dx^2} = M$$

and integrating equation (A4) give

$$EI\frac{dy}{dx} = M_1x - \frac{(1 - K_1)Px^2}{2} + C_1 \qquad 0 \le x \le a \tag{A6}$$

Integrating equation (A5) gives

$$EI\frac{dy}{dx} = M_1x + \frac{K_2Px^2}{2} - Pax + C_2 \qquad a \le x \le a + b \tag{A7}$$

Integrating equation (A6) results in

$$EIy = \frac{M_1x^2}{2} - \frac{(1 - K_1)Px^3}{6} + C_1x + C_3 \qquad 0 \le x \le a \tag{A8}$$

Integrating equation (A7) results in

$$EIy = \frac{M_1x^2}{2} + \frac{K_1Px^3}{6} - \frac{Pax^2}{2} + C_2x + C_4 \qquad a \le x \le a + b \tag{A9}$$

Applying boundary condition (1) to equation (A6) gives

$$EI\theta = C_1 \tag{A10}$$

Applying boundary condition (4) to equation (A7) gives

$$EI\theta = M_1(a + b) + \frac{K_1P(a + b)^2}{2} - Pa(a + b) + C_2 \tag{A11}$$

Applying boundary condition (2) to equation (A8) gives

$$EI(\delta_b - \delta_a) = C_3 \tag{A12}$$

Applying boundary condition (3) to equations (A8) and (A9) results in

$$EI\delta_b = \frac{M_1a^2}{2} - \frac{(1 - K_1)Pa^3}{6} + C_1a + C_3 \tag{A13}$$

$$EI\delta_b = \frac{M_1 a^2}{2} + \frac{K_1 P a^3}{6} - \frac{Pa^3}{2} + C_2 a + C_4 \tag{A14}$$

Applying boundary condition (5) to equation (A9) yields

$$0 = \frac{M_1 (a+b)^2}{2} + \frac{K_2 P (a+b)^3}{6} - \frac{Pa\,(a+b)^2}{2} + C_2\,(a+b) + C_4 \tag{A15}$$

From equations (A10), (A12), and (A13)

$$0 = \frac{M_1}{2}(a+b)^2 + \frac{K_2 P}{6}(a+b)^3 - \frac{P}{6}(a^3 + 6a^2 b + 3ab^2) + C_2 b + EI\theta a + EI(\delta_b - \delta_a) \tag{A16}$$

From boundary condition (6) and equations (A6) and (A7)

$$C_2 = EI\theta + \frac{Pa^2}{2} \tag{A17}$$

From equations (A11) and (A17)

$$M_1 = -\frac{K_1 P}{2}(a+b) + \frac{Pa(a+2b)}{2(a+b)} \tag{A18}$$

Combining equations (A16), (A17), and (A18) and substituting $\delta_b - \delta_a = \theta l$ into the result yield

$$EI\theta(a+b+l) - \frac{K_1 P}{12}(a+b)^3 + \frac{Pa^2}{12}(a+3b) = 0 \tag{A19}$$

Finally, from equations (A3) and (A19)

$$EI\theta = \frac{P}{12}\,\frac{(a+b)^3\,(l+a-S_2) - a^2\,(a+3b)(a+b+l)}{(a+b+l)^2} \tag{A20}$$

The axial stiffness of the pad mount K_m is

$$K_m = \frac{P}{\frac{\delta_a + \delta_b}{2}} \tag{A21}$$

From equations (A14), (A15), (A17), and (A18)

$$EI\delta_b = \frac{K_1 P(b^3 + 3ab^2)}{12} - \frac{Pa^2b^2}{4(a + b)} - EI\theta b \tag{A22}$$

From equations (A16) and (A18)

$$EI\delta_a = -\frac{K_1 P(a^3 + 3a^2b)}{12} + \frac{Pa^3(a + 4b)}{12(a + b)} + EI\theta a \tag{A23}$$

From equations (A3), (A20), (A22), and (A23)

$$\frac{\delta_a + \delta_b}{2} = \frac{P}{24EI}\left[\frac{(b - a)(b^2 + 4ab + a^2)(l + a - S_2) + a^2(b - a)(a + 3b)}{a + b + l}\right.$$

$$\left. - \frac{(b - a)(a + b)^3(l + a - S_2)}{(a + b + l)^2} + \frac{a^2(a^2 + 4ab - 3b^2)}{a + b}\right] \tag{A24}$$

Equations (A20), (A21), and (A24) are used in conjunction with the compressible-flow solution for a flat slider to obtain the operating characteristics of the pad.

APPENDIX B

DERIVATION OF PAD SUPPORT BEAM DEFLECTION AND AXIAL STIFFNESS FOR CONSTRAINED SUPPORTS

From figure 2 the boundary conditions are

(1) At $x = 0$, $dy/dx = \theta$.

(2) At $x = 0$, $y = \delta_b - \delta_a$.

(3) At $x = a$, $dy/dx = 0$.

(4) At $x = a$, $y = \delta_b$.

(5) At $x = a + b$, $dy/dx = \theta$.

(6) At $x = a + b$, $y = 0$.

For the beam from $x = 0$ to $x = a$

$$M = M_4 - (1 - K_2)Px \tag{B1}$$

$$M_{5L} + M_4 - (1 - K_2)Pa = 0 \tag{B1a}$$

For the beam from $x = a$ to $x = a + b$

$$M = M_3 - (a + b - x)K_2P \tag{B2}$$

$$M_{5R} + M_3 - K_2Pb = 0 \tag{B2a}$$

Using the beam equation and integrating equation (B1) result in

$$EI\frac{dy}{dx} = M_4x - (1 - K_2)\frac{Px^2}{2} + C_1 \qquad 0 \le x \le a \tag{B3}$$

Integrating equation (B2) gives

$$EI\frac{dy}{dx} = M_3x - (a + b)K_2Px + \frac{K_2Px^2}{2} + C_2 \qquad a \le x \le a + b \tag{B4}$$

Integrating equation (B3) yields

$$EIy = \frac{M_4x^2}{2} - \frac{(1 - K_2)Px^3}{6} + C_1x + C_3 \qquad 0 \le x \le a \tag{B5}$$

Integrating equation (B4) yields

$$EIy = \frac{M_3 x^2}{2} - \frac{(a+b)K_2}{2} Px^2 + \frac{K_2}{6} Px^3 + C_2 x + C_4 \qquad a \le x \le a+b \tag{B6}$$

Applying boundary condition (1) to equation (B3) results in

$$EI\theta = C_1 \tag{B7}$$

Applying boundary condition (3) to equation (B3) results in

$$M_4 a - (1 - K_2)\frac{Pa^2}{2} + EI\theta = 0 \tag{B8}$$

Applying boundary condition (3) to equation (B4) results in

$$M_3 a - a\left(\frac{a}{2} + b\right) K_2 P + C_2 = 0 \tag{B9}$$

Applying boundary condition (5) to equation (B4) gives

$$EI\theta = M_3(a+b) - \frac{(a+b)^2}{2} K_2 P + C_2 \tag{B10}$$

Applying boundary condition (2) to equation (B5) gives

$$EI(\delta_b - \delta_a) = C_3 \tag{B11}$$

Applying boundary condition (4) to equation (B5) yields

$$EI\delta_b = \frac{M_4 a^2}{2} - \frac{(1 - K_2)}{6} a^3 P + C_1 a + C_3 \tag{B12}$$

Applying boundary condition (4) to equation (B6) yields

$$EI\delta_b = \frac{M_3 a^2}{2} - a^2\left(\frac{a}{3} + \frac{b}{2}\right) K_2 P + C_2 a + C_4 \tag{B13}$$

Applying boundary condition (6) to equation (B6) gives

$$0 = \frac{M_3(a+b)^2}{2} - \frac{(a+b)^3 K_2 P}{3} + C_2(a+b) + C_4 \tag{B14}$$

Substituting equations (B7) and (B11) and the value of M_4 from equation (B8) into (B12) yields

$$\frac{a^3(1-K_2)P}{12} + \frac{EI\theta a}{2} + EI(\delta_b - \delta_a) - EI\delta_b = 0 \tag{B15}$$

Eliminating C_2 from equations (B9) and (B10) yields

$$EI\theta = M_3 b - \frac{b^2 K_2}{2} P \tag{B16}$$

Eliminating C_2 and C_4 from equations (B9), (B13), and (B14) gives

$$\frac{M_3 b^2}{2} - \frac{b^3}{3} K_2 P + EI\delta_b = 0 \tag{B17}$$

Eliminating M_3 from equations (B16) and (B17) yields

$$\frac{b^3 K_2 P}{12} - \frac{EI\theta b}{2} - EI\delta_b = 0 \tag{B18}$$

Combining equations (B15) and (B18) and setting $\delta_b - \delta_a = \theta l$ yield

$$EI\theta = \frac{P\left[(a^3 + b^3)K_2 - a^3\right]}{6(a + b + 2l)} \tag{B19}$$

For the pad (fig. 3(c))

$$K_2 P S_2 + M_3 - M_4 - (1 - K_2)(l - S_2)P = 0 \tag{B20}$$

Combining equations (B8), (B16), and (B20) yields

$$K_2 = \frac{a + 2l - 2S_2}{a + b + 2l} - \frac{2EI\theta(a + b)}{Pab(a + b + 2l)} \tag{B21}$$

From equations (B19) and (B21)

$$EI\theta = \frac{Pab\left[(a^3 + b^3)(a + 2l - 2S_2) - a^3(a + b + 2l)\right]}{2\left[(a + b)(a^3 + b^3) + 3ab(a + b + 2l)^2\right]} \tag{B22}$$

From equations (B15), (B18), (B21), and (B22)

$$\frac{\delta_a + \delta_b}{2} = \frac{P}{24EI}\left\{\frac{a^3b + b^3a + 2b^3l - 2S_2(b^3 - a^3)}{a + b + 2l}\right.$$

$$\left. - \frac{(b - a)(b^3 + 5a^2b + 5ab^2 + a^3 + 6abl)\left[(a^3 + b^3)(a + 2l - 2S_2) - a^3(a + b + 2l)\right]}{(a + b + 2l)\left[(a + b)(a^3 + b^3) + 3ab(a + b + 2l)^2\right]}\right\} \tag{B23}$$

Equations (B22), (B23), and (A21) are used in conjunction with the compressible-flow solution for a flat slider to obtain the operating characteristics of the pad.

REFERENCES

1. Barnum, T.; and Elrod, H. G., Jr.: An Experimental Study of the Dynamic Behavior of Foil Bearings. ASME Trans. J. of Lub. Tech., vol. 94, ser. F, no. 1, Jan. 1972, pp. 93-100.

2. Licht, L.: The Dynamic Characteristics of a Turborotor Simulator Supported on Gas Lubricated Foil Bearings; Part 3: Rotation in Foil Bearings of Reduced Length, With Starting and Stopping Unaided by External Pressurization. ASME Trans. J. of Lub. Tech., vol. 94, ser. F, no. 3, July 1972, pp. 211-222.

3. Licht, L.; Branger, M.; and Anderson, W. J.: Gas-Lubricated Foil Bearings for High Speed Turboalternator - Construction and Performance. Paper 73-LUB-5, ASME, Oct. 1973.

4. Barnett, M. A.; and Silver, A.: Application of Air Bearings to High-Speed Turbomachinery. Paper 700720, SAE, Sept. 1970.

5. Annis, B. B.: Cutless Rubber Bearings. Mar. Eng. Ship. Age, vol. 32, no. 5, May 1927, pp. 275-277.

6. Fogg, A.; and Hunwick, S. A.: Some Experiments with Water Lubricated Rubber Bearings. General Discussions on Lubrication and Lubricants. Proc. Inst. Mech. Eng., vol. 1, 1937, pp. 101-106.

7. Castelli, V.; Rightmire, G. K.; and Fuller, D. D.: On the Analytical and Experimental Investigation of a Hydrostatic, Axisymmetric Compliant-Surface Thrust Bearing. ASME Trans. J. of Lub. Tech., vol. 89, ser. F., no. 4, Oct. 1967, pp. 510-520.

8. Benjamin, M. K.; and Castelli, V.: A Theoretical Investigation of Compliant Surface Journal Bearings. ASME Trans. J. of Lub. Tech., vol. 93, ser. F, no. 1, Jan. 1971, pp. 191-201.

9. Pirvics, J.; and Castelli, V.: Elastomer Viscoelasticity Effects in Compliant Surface Bearings. ASME Trans. J. Lub. Tech., vol. 95, ser. F, no. 3, Jul. 1973, pp. 363-371.

10. Pirvics, J.; and Castelli, V.: Elastomer Inertia Effects in Compliant Surface Bearings. ASME Trans. J. of Lub. Tech., vol. 95, ser. F, no. 3, Jul. 1973, pp. 372-380.

11. Dayson, Clive: Flexible Stepped Thrust Bearings. ASLE Trans., vol. 16, no. 1, Jan. 1973, pp. 32-41.

12. Rieger, N., ed.: Design of Gas Bearings. Rensselaer Polytechnic Institute and Mechanical Technology, Inc., 1967.

TABLE I. - OPTIMUM OPERATING CONDITIONS FOR RESILIENT-PAD BEARING WITH CONSTRAINED SUPPORTS

[Young's modulus of beam material, 3.47×10^{11} N/m^2 (50×10^6 psi).]

(a) Bearing characteristic number, 1; film thickness ratio, 2.45; location of center of pressure on pad, 0.605; pad load, 0.434 newton (0.0975 lb)

Length ratio, b/a	Thickness of flexible beam, t		Film thickness at exit from pad, h_2		Rotative speed of slider, N, rpm	Flexible beam stiffness, K_m	
						N/m	lb/in.
	mm	in.	μm	μin.			
1.2	0.127	0.005	0.965	38	12	4.11×10^4	235
	.254	.010	.13	5	.2	3.28×10^5	1 875
	.508	.020	.015	.6	.003	2.62×10^6	15 000
1.4	0.127	0.005	2.87	113	108	4.15×10^4	237
	.254	.010	.361	14.2	1.7	3.31×10^5	1 890
	.508	.020	.0051	.2	.0003	2.64×10^6	15 100
1.6	0.127	0.005	4.47	176	259	4.15×10^4	237
	.254	.010	.559	22	4	3.31×10^5	1 890
	.508	.020	.069	2.7	.06	2.64×10^6	15 100
1.8	0.127	0.005	5.76	227	434	4.13×10^4	236
	.254	.010	.71	28	6.6	3.29×10^5	1 880
	.508	.020	.091	3.6	.1	2.64×10^6	15 100
2.0	0.127	0.005	6.88	271	616	4.07×10^4	233
	.254	.010	.863	34	9.7	3.27×10^5	1 870
	.508	.020	.11	4.2	.15	2.59×10^6	14 900

TABLE I. - Continued. OPTIMUM OPERATING CONDITIONS FOR

RESILIENT-PAD BEARING WITH CONSTRAINED SUPPORTS

[Young's modulus of beam material, 3.47×10^{11} N/m^2 (50×10^6 psi).]

(b) Bearing characteristic number, 10; film thickness ratio, 2.60; location of center of pressure on pad, 0.640; pad load, 4.05 newtons (0.91 lb)

Length ratio, b/a	Thickness of flexible beam, t		Film thickness at exit from pad, h_2		Rotative speed of slider, N, rpm	Flexible beam stiffness, K_m	
	mm	in.	μm	μin.		N/m	lb/in.
1.2	0.127	0.005	3.99	157	2 070	4.14×10^4	237
	.254	.010	.432	17	24.3	3.32×10^5	1 900
	.508	.020	.061	2.4	.5	2.66×10^6	15 200
1.4	0.127	0.005	20.1	789	52 300	4.23×10^4	242
	.254	.010	2.51	99	819	3.39×10^5	1 940
	.508	.020	.305	12	12.8	2.71×10^6	15 500
1.6	0.127	0.005	33	1300	142 000	4.27×10^4	244
	.254	.010	4.14	163	2 240	3.41×10^5	1 950
	.508	.020	.508	20	33.6	2.73×10^6	15 600
1.8	0.127	0.005	43.9	1730	251 000	4.27×10^4	244
	.254	.010	5.43	216	3 930	3.41×10^5	1 950
	.508	.020	.686	27	61.4	2.73×10^6	15 600
2.0	0.127	0.005	52.8	2080	365 000	4.27×10^4	244
	.254	.010	6.6	260	5 700	3.41×10^5	1 950
	.508	.020	.838	33	91	2.73×10^6	15 600

TABLE I. - Concluded. OPTIMUM OPERATING CONDITIONS FOR RESILIENT-PAD BEARING WITH CONSTRAINED SUPPORTS

[Young's modulus of beam material, 3.47×10^{11} N/m^2 (50×10^6 psi).]

(c) Bearing characteristic number, 40; film thickness ratio, 3.6; location of center of pressure on pad, 0.695; pad load, 11.5 newtons (2.58 lb)

Length ratio, b/a	Thickness of flexible beam, t		Film thickness at exit from pad, h_2		Rotative speed of slider, N, rpm	Flexible beam stiffness, K_m	
	mm	in.	μm	μin.		N/m	lb/in.
1.2	0.127 .254 .508	0.005 .010 .020	(a)	(a)	(a)	(a)	(a)
1.4	0.127 .254 .508	0.005 .010 .020	23.1 2.9 .361	908 114 14.2	277 000 4 340 67.8	4.39×10^4 3.5×10^5 2.8×10^6	251 2 000 16 000
1.6	0.127 .254 .508	0.005 .010 .020	45.1 5.64 .711	1775 222 28	1 060 000 16 600 263	4.48×10^4 3.58×10^5 2.87×10^6	256 2 050 16 400
1.8	0.127 .254 .508	0.005 .010 .020	63.0 7.87 .99	2480 310 39	2 070 000 32 400 512	4.55×10^4 3.64×10^5 2.90×10^6	260 2 080 16 600
2.0	0.127 .254 .508	0.005 .010 .020	77.8 9.72 1.22	3065 383 48	3 150 000 49 400 772	4.58×10^4 3.66×10^5 2.92×10^6	262 2 090 16 700

[a]Negative slopes.

TABLE II. - OPTIMUM OPERATING CONDITIONS FOR RESILIENT-PAD BEARING WITH SIMPLE SUPPORTS

[Young's modulus of beam material, 3.47×10^{11} N/m^2 (50×10^6 psi).]

(a) Bearing characteristic number, 1; film thickness ratio, 2.45; location of center of pressure on pad, 0.605; pad load, 0.434 newton (0.0975 lb)

Length ratio, b/a	Thickness of flexible beam, t		Film thickness at exit from pad, h_2		Rotative speed of slider, N, rpm	Flexible beam stiffness, K_m	
	mm	in.	μm	μin.		N/m	lb/in.
1.2	0.127	0.005	(a)	(a)	(a)	(a)	(a)
	.254	.010					
	.508	.020					
1.4	0.127	0.005	1.83	72	43	4.16×10^4	238
	.254	.010	.23	9	.67	3.34×10^5	1 910
	.508	.020	.028	1.1	.01	2.66×10^6	15 200
1.6	0.127	0.005	3.73	147	182	4.16×10^4	238
	.254	.010	.46	18	2.73	3.32×10^5	1 900
	.508	.020	.058	2.3	.04	2.66×10^6	15 200
1.8	0.127	0.005	5.31	209	368	4.14×10^4	237
	.254	.010	.66	26	5.7	3.31×10^5	1 890
	.508	.020	.084	3.3	.09	2.64×10^6	15 100
2.0	0.127	0.005	6.60	260	570	4.09×10^4	234
	.254	.010	.838	33	8.9	3.27×10^5	1 870
	.508	.020	.103	4.1	.14	2.62×10^6	15 000

[a]Negative slopes.

TABLE II. - Continued. OPTIMUM OPERATING CONDITIONS FOR

RESILIENT-PAD BEARING WITH SIMPLE SUPPORTS

[Young's modulus of beam material, 3.47×10^{11} N/m^2 (50×10^6 psi).]

(b) Bearing characteristic number, 10; film thickness ratio, 2.60; location of center of pressure on pad, 0.640; pad load, 4.05 newtons (0.91 lb)

Length ratio, b/a	Thickness of flexible beam, t		Film thickness at exit from pad, h_2		Rotative speed of slider, N, rpm	Flexible beam stiffness, K_m	
	mm	in.	μm	μin.		N/m	lb/in.
1.2	0.127	0.005	(a)	(a)	(a)	(a)	(a)
	.254	.010					
	.508	.020					
1.4	0.127	0.005	5.79	228	4 370	4.28×10^4	245
	.254	.010	.736	29	70.6	3.43×10^5	1 960
	.508	.020	.091	3.6	1.1	2.73×10^6	15 600
1.6	0.127	0.005	22.0	867	63 100	4.32×10^4	247
	.254	.010	2.74	108	980	3.45×10^5	1 970
	.508	.020	.345	13.6	15.4	2.76×10^6	15 800
1.8	0.127	0.005	35.3	1390	163 000	4.32×10^4	247
	.254	.010	4.42	174	2 550	3.45×10^5	1 970
	.508	.020	.558	22	40.7	2.76×10^6	15 800
2.0	0.127	0.005	46.2	1820	280 000	4.30×10^4	246
	.254	.010	5.79	228	4 380	3.45×10^5	1 970
	.508	.020	.736	29	70.6	2.75×10^6	15 700

[a]Negative slopes.

TABLE II. - Concluded. OPTIMUM OPERATING CONDITIONS FOR

RESILIENT-PAD BEARING WITH SIMPLE SUPPORTS

[Young's modulus of beam material, 3.47×10^{11} N/m^2 (50×10^6 psi).]

(c) Bearing characteristic number, 40; film thickness ratio, 3.6; location of center of pressure on pad, 0.695; pad load, 11.5 newtons (2.58 lb)

Length ratio, b/a	Thickness of flexible beam, t		Film thickness at exit from pad, h_2		Rotative speed of slider, N, rpm	Flexible beam stiffness, K_m	
	mm	in.	μm	μin.		N/m	lb/in.
1.2	0.127	0.005	(a)	(a)	(a)	(a)	(a)
	.254	.010					
	.508	.020					
1.4	0.127	0.005	(a)	(a)	(a)	(a)	(a)
	.254	.010					
	.508	.020					
1.6	0.127	0.005	12.1	476	76 100	4.58×10^4	262
	.254	.010	1.52	60	1 210	3.66×10^5	2 090
	.508	.020	.19	7.4	18.6	2.92×10^6	16 700
1.8	0.127	0.005	35.3	1390	650 000	4.65×10^4	266
	.254	.010	4.42	175	10 200	3.71×10^5	2 120
	.508	.020	.56	22	162	2.97×10^6	17 000
2.0	0.127	0.005	54.6	2150	1 550 000	4.67×10^4	267
	.254	.010	6.83	269	24 200	3.74×10^5	2 140
	.508	.020	.85	33.6	379	2.99×10^6	17 100

[a]Negative slopes.

TABLE III. - OPERATING CHARACTERISTICS OF RESILIENT-PAD BEARING AT PAD LOADING OF 1.12×10^4 NEWTONS PER SQUARE METER (1.62 PSI)

[Length ratio, 1.7; thickness of flexible beam, 0.254 mm (0.010 in.); Young's modulus of beam material, 3.47×10^{11} N/m^2 (50×10^6 psi).]

Bearing characteristic number, Λ	Film thickness ratio, h_1/h_2	Location of center of pressure on pad, S_2/l	Simple supports					Constrained supports				
			Film thickness at exit from pad, h_2		Rotative speed of slider, N, rpm	Flexible beam stiffness, K_m		Film thickness at exit from pad, h_2		Rotative speed of slider, N, rpm	Flexible beam stiffness, K_m	
			μm	μin.		N/m	lb/in.	μm	μin.		N/m	lb/in.
20	7.80	0.750	(a)	(a)	(a)	(a)	(a)	0.686	27	123	3.84×10^5	2190
15	5.90	.710	0.41	16	31	3.76×10^5	2150	1.2	47	280	3.67	2100
10	2.60	.640	3.64	143	1 720	3.47	1980	4.84	190	3 030	3.41	1950
15	1.60	.620	11.5	453	25 900	3.38	1930	13.9	545	37 400	3.36	1920
20	1.40	.620	17.3	680	77 600	3.38	1930	20.8	817	112 000	3.36	1920
25	1.40	.630	15.9	625	82 200	3.41	1950	20.1	791	131 000	3.38	1930

[a]Negative slope.

TABLE IV. - OPERATING CHARACTERISTICS OF RESILIENT-PAD BEARING AT PAD LOADING OF 2.63×10^4 NEWTONS PER SQUARE METER (3.79 PSI)

[Length ratio, 1.7; thickness of flexible beam, 0.254 mm (0.010 in.); Young's modulus of beam material, 3.47×10^{11} N/m^2 (50×10^6 psi).]

Bearing characteristic number, Λ	Film thickness ratio, h_1/h_2	Location of center of pressure on pad, S_2/l	Simple supports					Constrained supports				
			Film thickness at exit from pad, h_2		Rotative speed of slider, N, rpm	Flexible beam stiffness, K_m		Film thickness at exit from pad, h_2		Rotative speed of slider, N, rpm	Flexible beam stiffness, K_m	
			μm	μin.		N/m	lb/in.	μm	μin.		N/m	lb/in.
45	7.1	0.740	0.13	5	9	3.91×10^5	2230	1.93	76	2 180	3.80×10^5	2170
40	6.0	.730	.41	16	85	3.85	2200	2.5	98	3 200	3.75	2140
35	4.9	.710	1.17	46	620	3.76	2150	3.5	138	5 600	3.67	2100
30	3.1	.660	5.24	206	10 800	3.54	2020	8.04	316	25 200	3.48	1990
35	2.5	.670	6.48	255	19 200	3.59	2050	10.8	426	53 400	3.52	2010
40	2.25	.675	7.28	286	27 600	3.60	2060	12.8	501	84 500	3.54	2020
45	2.10	.680	7.67	302	34 600	3.62	2070	14.2	558	118 000	3.55	2030

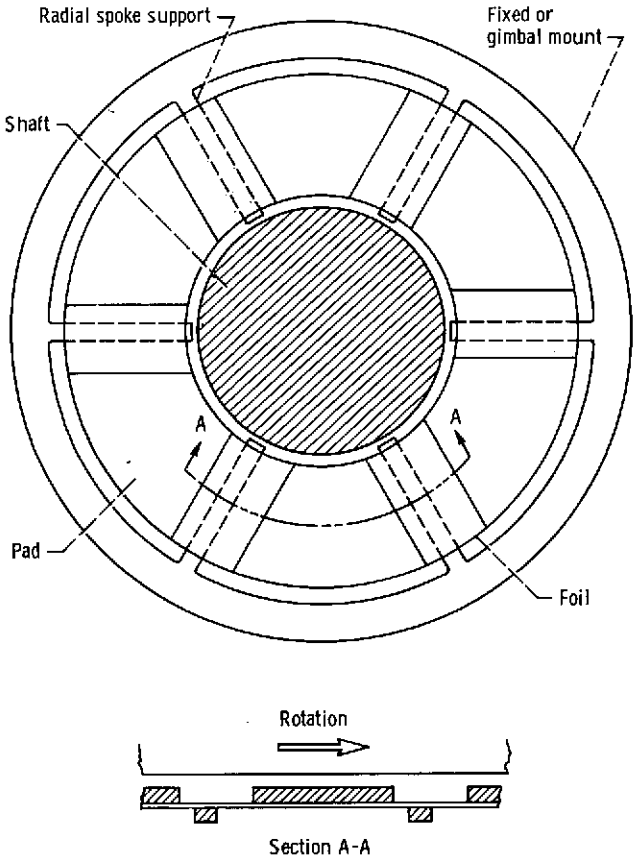

Figure 1. - Schematic of resilient-pad gas bearing.

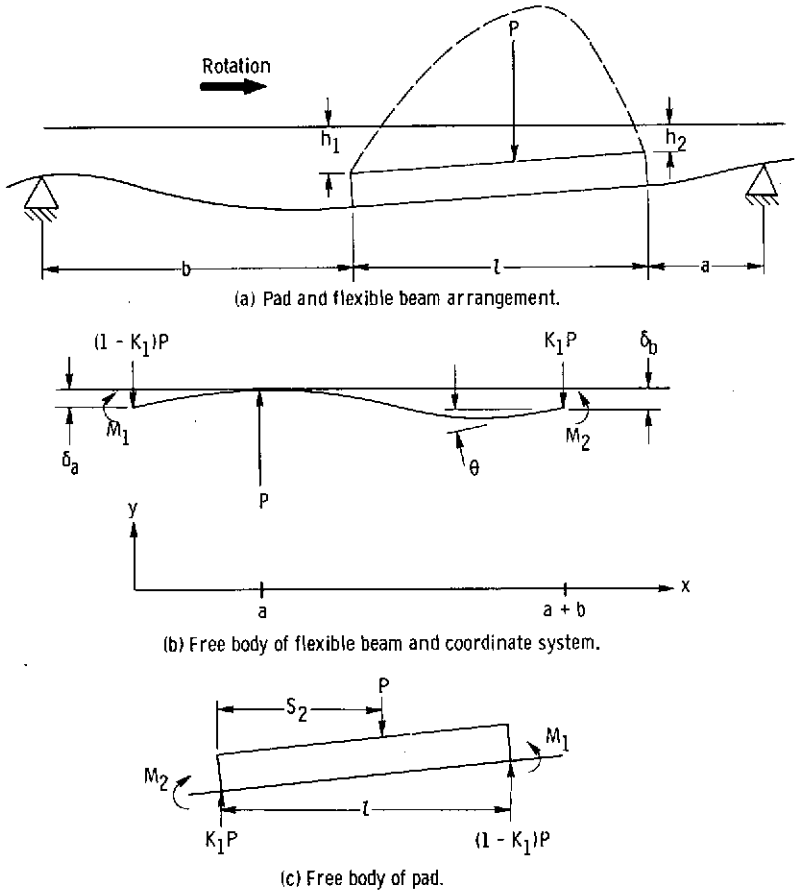

Figure 2. - Schematic of resilient-pad bearing with simple supports.

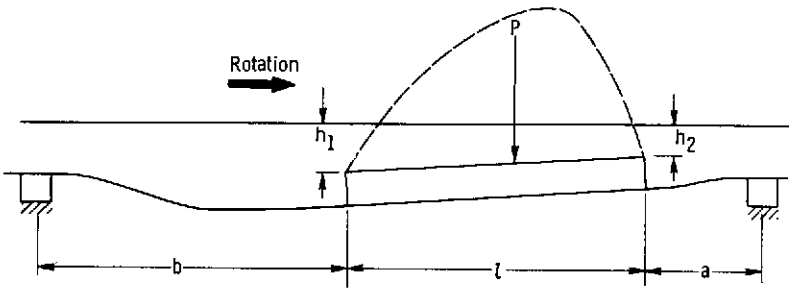

(a) Pad and flexible beam arrangement.

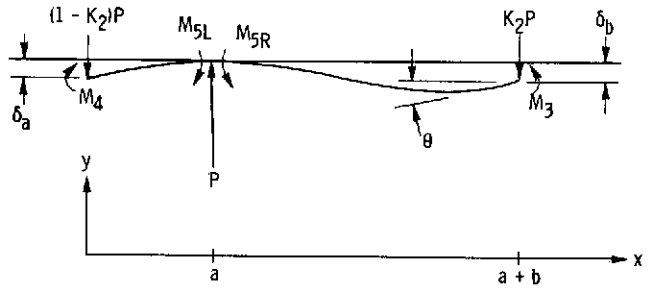

(b) Free body of flexible beam and coordinate system.

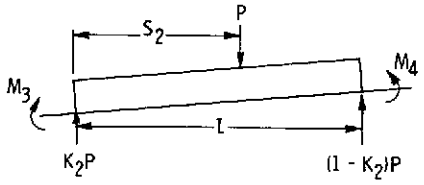

(c) Free body of pad.

Figure 3. - Schematic of resilient-pad bearing with constrained supports.

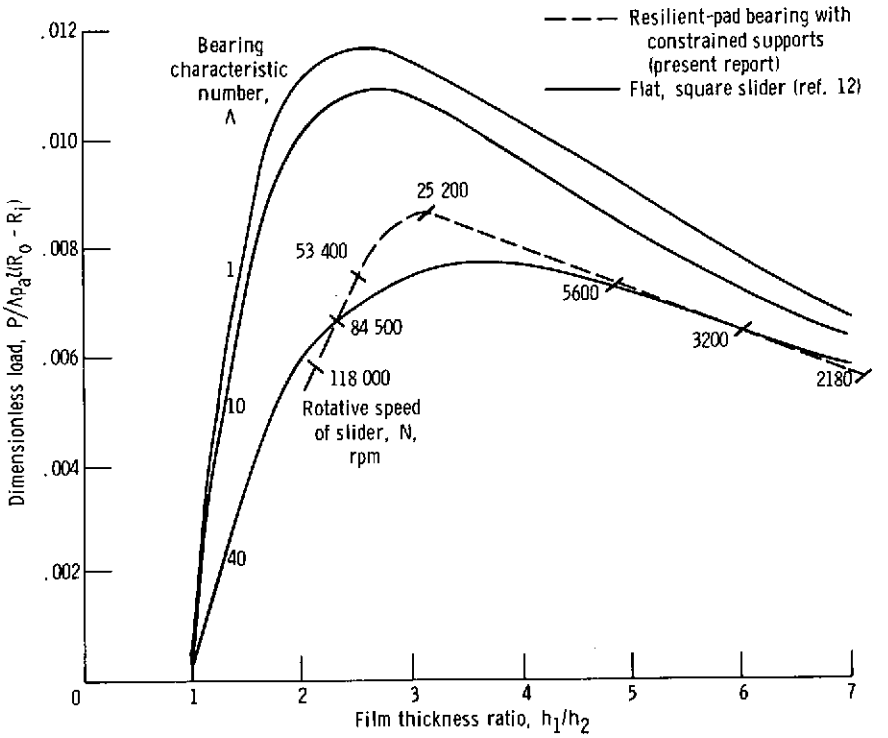

Figure 4. - Load capacity for flat, square slider at three values of bearing characteristic number and operating line for resilient-pad bearing designed for optimum load capacity at 25 000 rpm. Conditions for bearing: length ratio, 1.7; thickness of flexible beam, 0.254 millimeter (0.010 in.); Young's modulus of beam material, 3.47×10^{11} newtons per square meter (50×10^6 psi); pad load, 2.63×10^4 newtons per square meter (3.79 psi).

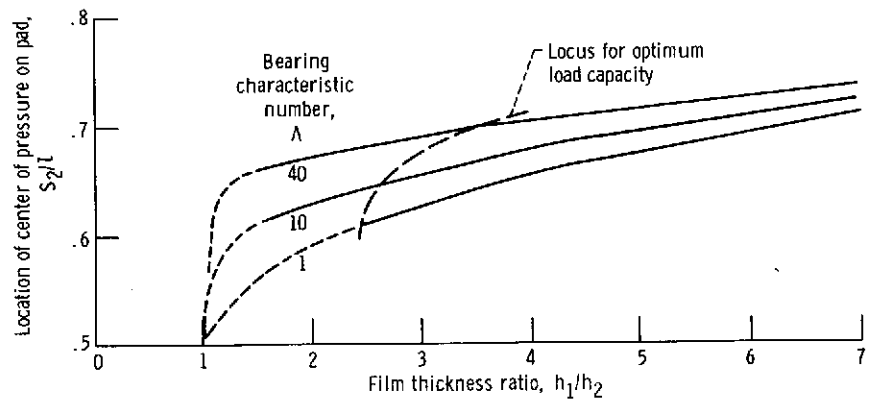

Figure 5. - Location of center of pressure as function of film thickness ratio and bearing characteristic number for flat, square slider (ref. 12).

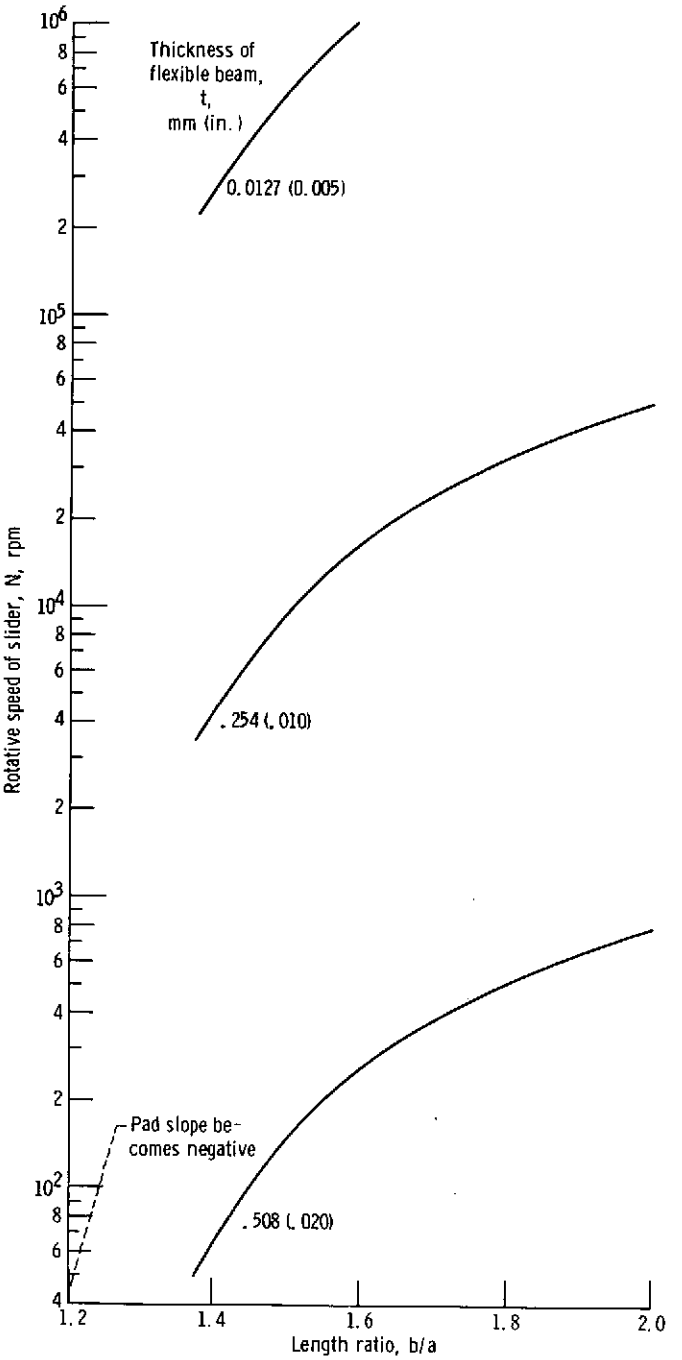

Figure 6. - Operating speeds for optimum load capacity at bearing characteristic number of 40 with three beam thicknesses. Constrained supports; pad load, 3.19×10^4 newtons per square meter (4.59 psi); Young's modulus of beam material, 3.47×10^{11} newtons per square meter (50×10^6 psi).

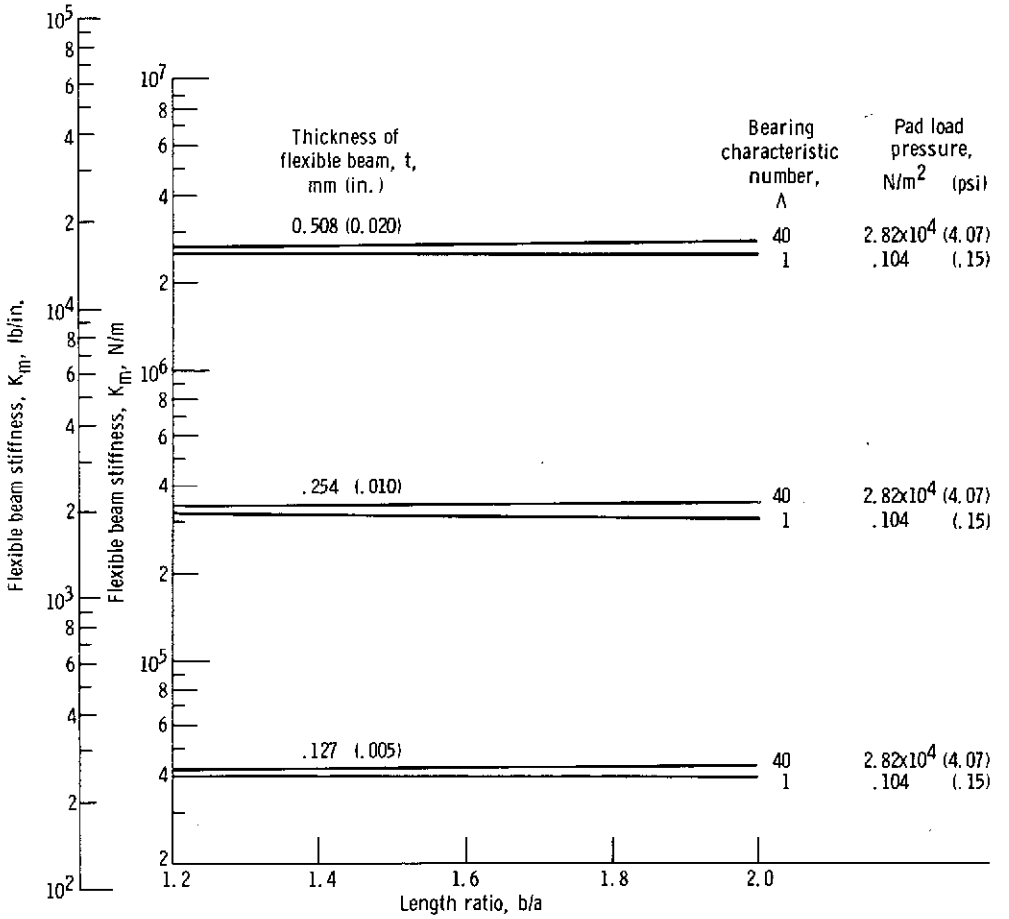

Figure 7. - Flexible beam stiffness as function of length ratio and beam thickness for resilient-pad bearing with constrained supports. Young's modulus of beam material, 3.47×10^{11} newtons per square meter (50×10^6 psi).

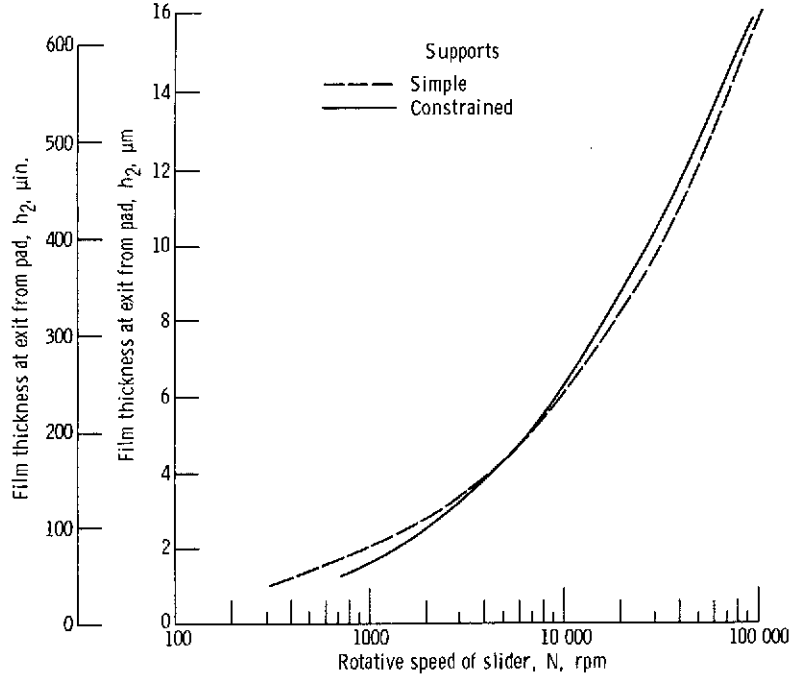

Figure 8. - Comparison of film thickness at exit from pad (minimum film thickness) for resilient-pad bearings with simple and constrained supports. Pad load, 1.96×10^4 newtons per square meter (2.83 psi); length ratio, 1.7; thickness of flexible beam, 0.254 millimeter (0.010 in.); Young's modulus of beam material, 3.47×10^{11} newtons per square meter (50×10^6 psi).

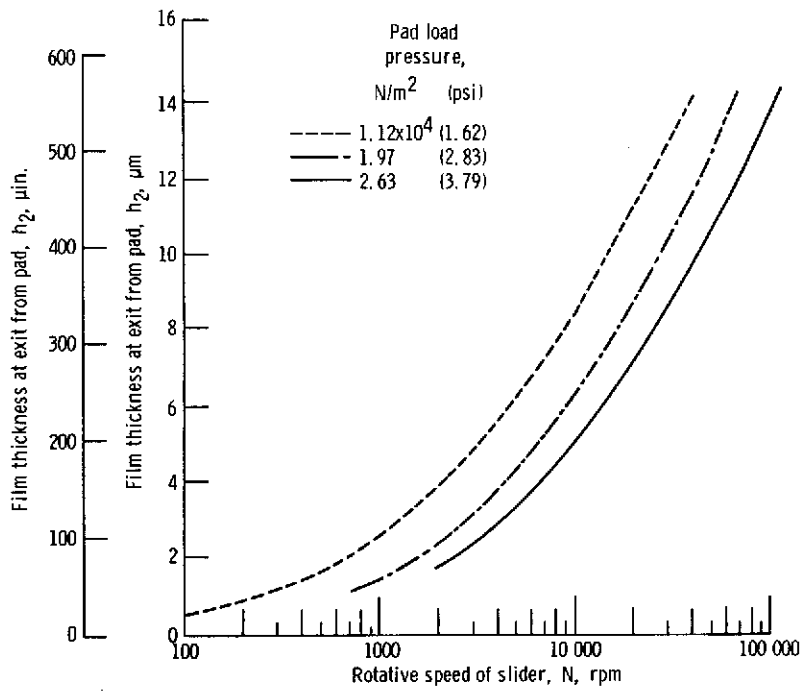

Figure 9. - Film thickness at exit from pad (minimum film thickness) as function of speed for resilient-pad bearing with constrained supports. Length ratio, 1.7; thickness of flexible beam, 0.254 centimeter (0.010 in.); Young's modulus of beam material, 3.47×10^{11} newtons per square meter (50×10^6 psi).

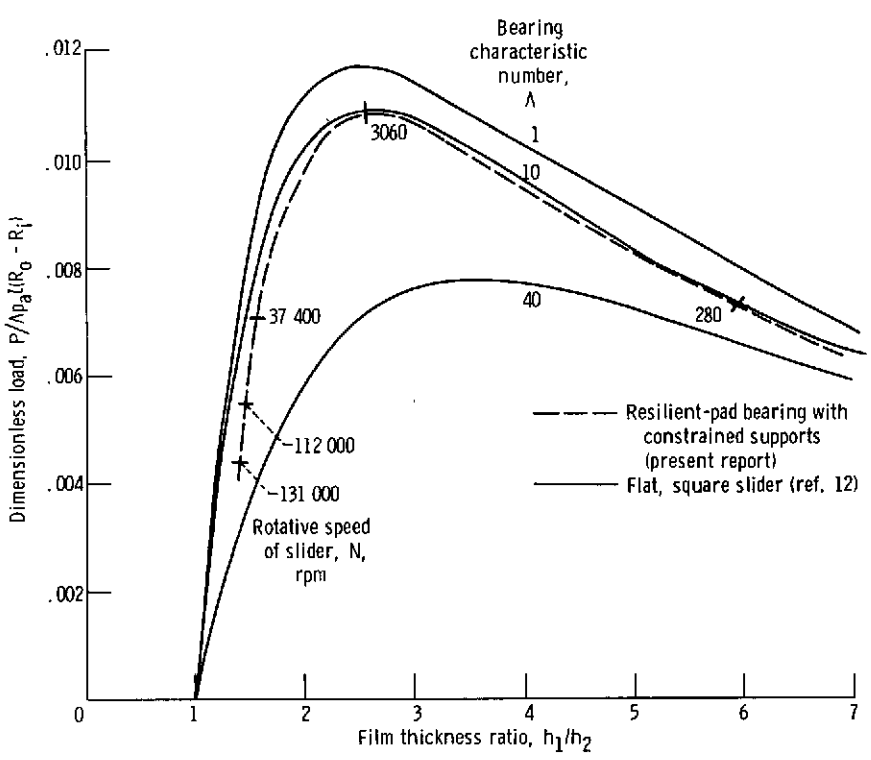

Figure 10. - Load capacity for flat, square slider at three values of bearing characteristic number and operating line for resilient-pad bearing designed for optimum load capacity at 3060 rpm. Conditions for bearing: length ratio, 1.7; thickness of flexible beam, 0.254 millimeter (0.010 in.); Young's modulus of beam material, 3.47×10^{11} newtons per square meter (50×10^6 psi); pad load, 1.12×10^4 newtons per square meter (1.62 psi).

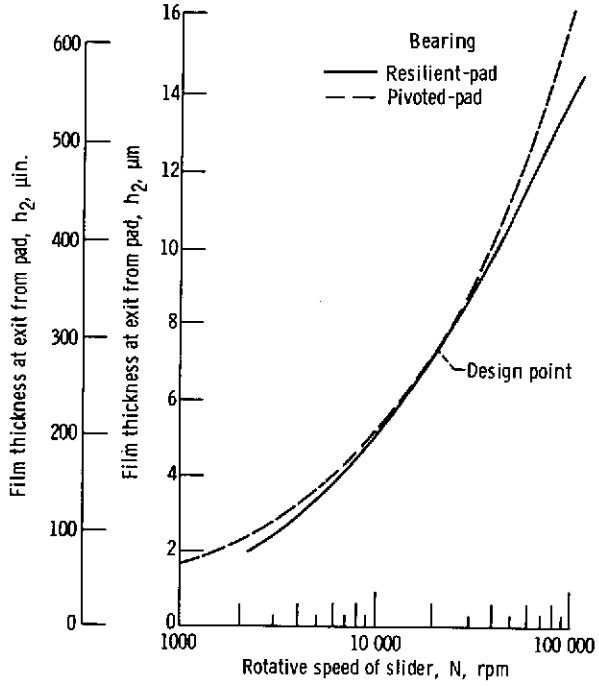

Figure 11. - Comparison of film thickness at exit from pad (minimum film thicknesses) for resilient-pad and pivoted-pad bearings. Pad load, 2.63×10^4 newtons per square meter (3.79 psi); pivot position of pivoted-pad bearing, 0.685; conditions for resilient-pad bearing: length ratio, 1.7; thickness of flexible beam, 0.254 millimeter (0.010 in.); Young's modulus of beam material, 3.47×10^{11} newtons per square meter (50×10^6 psi).